

Synthesis, Characterization, and Biological Affinity of a Near-Infrared-Emitting Conjugated Oligoelectrolyte

Alexander W. Thomas,[†] Zachary B. Henson,[†] Jenny Du,[†] Carol A. Vandenberg,[‡] and Guillermo C. Bazan^{*,†}

[†]Department of Chemistry & Biochemistry, and [‡]Department of Molecular, Cellular and Developmental Biology, University of California, Santa Barbara, California 93106, United States

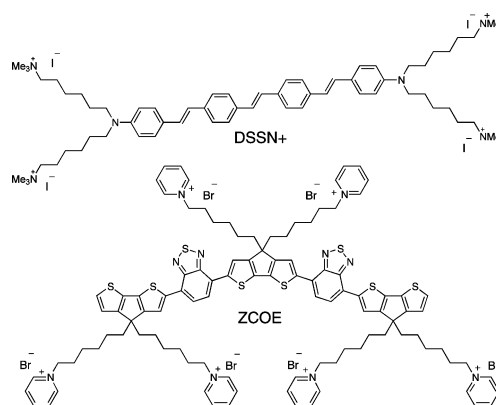
S Supporting Information

ABSTRACT: A near-IR-emitting conjugated oligoelectrolyte (COE), ZCOE, was synthesized, and its photophysical features were characterized. The biological affinity of ZCOE is compared to that of an established lipid-membrane-intercalating COE, DSSN+, which has blue-shifted optical properties making it compatible for tracking preferential sites of accumulation. ZCOE exhibits diffuse staining of *E. coli* cells, whereas it displays internal staining of select yeast cells which also show propidium iodide staining, indicating ZCOE is a “dead” stain for this organism. Staining of mammalian cells reveals complete internalization of ZCOE through endocytosis, as supported by colocalization with LysoTracker and late endosome markers. In all cases DSSN+ persists in the outer membranes, most likely due to its chemical structure more closely resembling a lipid bilayer.

Conjugated oligoelectrolytes (COEs) are a class of molecules containing a defined number of π -conjugated repeat units appended with ionic functionalities.¹ These molecules share many of the attractive properties of their more extensively studied polymeric counterparts, namely conjugated polyelectrolytes (CPEs), such as water solubility, delocalized electronic structure, and strong absorption profiles. As with CPEs, COEs find utility in organic electronic devices as electron injection layers¹ and photosensitizers,² in bioimaging applications,^{3–5} and in various biosensing schemes for polysaccharides,⁶ proteins,^{7–10} and bacteria.¹¹ COEs, however, possess certain unique properties vis-à-vis CPEs. In addition to being monodisperse, the tunable size and substituents of COEs allow for matching biologically relevant length scales and attributes. A prominent example of this is DSSN+, a linear oligophenylenevinylene with pendant ionic groups at the two termini of its long axis, that spontaneously intercalates into biological membranes, the structure of which is shown in Chart 1.¹²

DSSN+ and several structural analogues have been used to increase the performance of various bioelectronics systems, such as microbial fuel cells^{13–15} and microbial electrosynthesis devices.¹⁶ This increase in the flow of electron equivalents between microorganisms and electrodes is presumably due to favorable modification of the microbe–electrode interface. A clear membrane specificity for DSSN+ can be seen in bioimaging examples of bacteria¹⁴ and yeast.¹² Additionally,

Chart 1. COE Chemical Structures



DSSN+ and related COEs have been shown to increase ion conductance across mammalian membranes.¹⁷

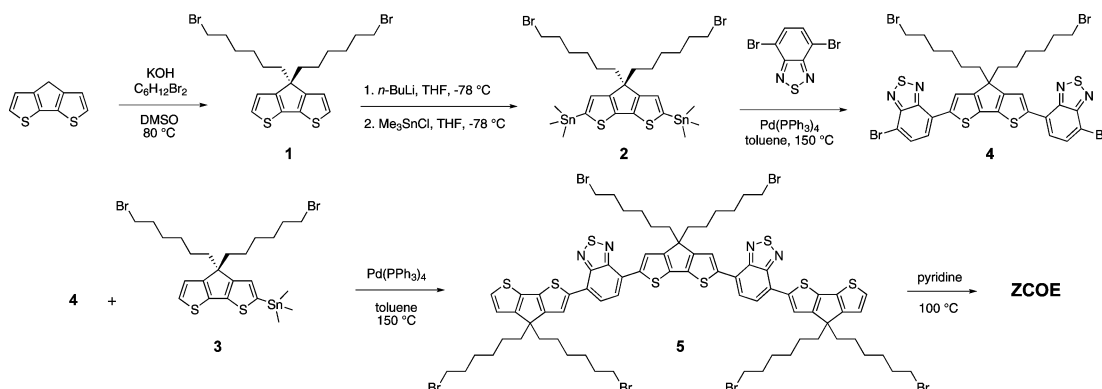
Studies have appeared that show how different COEs (and CPEs) exhibit different toxicity toward microorganisms.¹⁸ The ionic arrangement and density impact the biocidal activity and specific lipid affinity.^{19,20} While DSSN+ has not been studied extensively in this manner, evidence thus far suggests little to no biocidal or membrane-disrupting capacity at the concentrations useful for bioelectronics applications,¹⁶ perhaps due to a more membrane-compatible molecular design. To better understand the influence of molecular topology on the interactions of COEs with different cells, we present herein the synthesis, characterization, and biological affinity of a novel COE, ZCOE (Chart 1), with a topological distribution of ionic functionalities and red-shifted optical properties that allow one to differentiate its preferred cellular localization relative to the more established DSSN+.

The synthesis of ZCOE is shown in Scheme 1. Details are provided in the Supporting Information (SI). Briefly, deprotonation at the bridgehead position of cyclopentadithiophene (CDT), followed by reaction with 1,6-dibromohexane, affords compound 1. Treatment of 1 with 1 or 2 equiv of *n*-butyllithium, followed by treatment with Me₃SnCl, yields either the mono- (3) or bis-stannylated (2) compound. Stille coupling of 2 with 4,7-dibromobenzo[*c*][1,2,5]thiadiazole accesses the dibrominated species 4, which can then undergo another Stille

Received: December 13, 2013

Published: February 27, 2014

Scheme 1. Synthetic Preparation of ZCOE



coupling reaction with **3** to access the neutral precursor **5**. Treatment with pyridine generates **ZCOE**.

The photophysical features of **ZCOE** were probed via UV–vis absorption and photoluminescence spectroscopies in various solvents (Table 1). The neutral precursor **5** was used for

Table 1. Absorption Maximum (λ_{abs}), Molar Extinction Coefficient (ϵ), Emission Maximum (λ_{em}), and Quantum Yield (Φ) of **5 and **ZCOE** in Different Solvents**

	solvent			
	toluene ^a	chloroform ^a	methanol	water
λ_{abs} , nm	633	637	620	630
ϵ^b	7.6	7.8	5.6	4.1
λ_{em} , nm	722	758	n/a ^c	n/a ^d
Φ , %	4.7	2.6	0.4	n/a ^d

^aCompound **5** used due to solubility considerations. ^bL mol⁻¹ cm⁻¹ × 10⁻⁴. ^c λ_{em} not determined due to high signal-to-noise. ^dNo detectable emission in water.

characterization in toluene and chloroform. The spectra are available in the SI. Overall, one finds a broad, low-energy absorption from ~500 to 800 nm and a sharp, high-energy band from ~350 to 450 nm, with minimal solvatochromatic effects. The photoluminescence spectra of **ZCOE** exhibit a weak, broad, and featureless emission band stretching from ~650 to 1000 nm. The emission maximum exhibits a 36 nm hypsochromic shift as solvent polarity decreases from chloroform (758 nm) to toluene (722 nm) and is accompanied by an increase in quantum yield (Φ) from ~3% to ~5%. Low Φ values are typical for dyes that emit in this range,²¹ as anticipated by the energy gap law.²² It is worth pointing out that molecular design principles borrowed from organic optoelectronics give **ZCOE** its red-shifted optical attributes. More specifically, a modular approach of alternating electron-rich/electron-donating cyclopentadithiophene and electron-poor/electron-accepting benzothiadiazole building blocks has previously resulted in broad, red-shifted absorption profiles due to charge transfer between donor and acceptor units.²³

To visualize the interaction of **ZCOE** with a common bacterium and compare it to **DSSN+**, *E. coli* cells were incubated for 20 min with 5 μM **ZCOE** and **DSSN+** and examined by confocal microscopy (Figure 1). Spectral separation of the two chromophores is achieved due to the far-red absorption (optimally excited by a 635 nm laser) and near-IR emission of **ZCOE** in contrast to the more blue-shifted optical attributes of **DSSN+**, which is excited by a 405 nm laser.

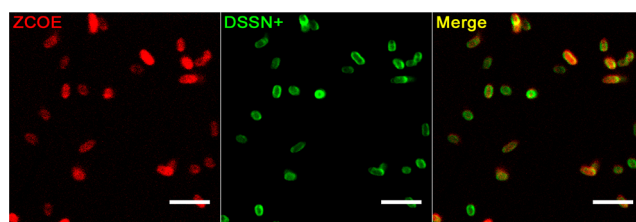


Figure 1. Single-plane confocal micrograph of *E. coli* cells stained with 5 μM **ZCOE** and **DSSN+**. Scale bars are 5 μm .

Both COEs present cell-specific emission with no background fluorescence due to their low quantum yields in polar media. Emission from **ZCOE** is mostly diffuse and featureless, plausibly due to an electrostatic association with the negatively charged bacterial surface,²⁴ which is in contrast to the “halo” pattern of **DSSN+** around the edges of the cells, consistent with membrane intercalation.

Subsequent selectivity experiments by confocal microscopy involved yeast cells that were incubated for 20 min with 5 μM **ZCOE**. In contrast to the indiscriminate staining of *E. coli*, **ZCOE** displays bright intracellular fluorescence in only certain yeast cells (Figure 2, top). These same cells are also stained by propidium iodide (PI), a membrane-impermeable dye that binds DNA, commonly used as an indicator of membrane permeability or “dead” stain.²⁵ Extensive colocalization of the

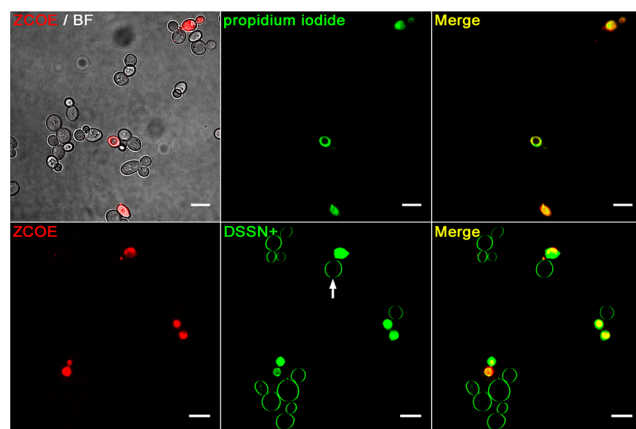


Figure 2. Two single-plane confocal and bright-field (BF) micrographs of yeast cells stained with 5 μM **ZCOE**, propidium iodide (top), and **DSSN+** (bottom). Arrow indicates axial attenuated emission from **DSSN+** when illuminated by the polarized light.⁴ Scale bars are 10 μm .

two dyes is observed: 82% (37 of 45) of cells displaying ZCOE fluorescence also display PI fluorescence, and 93% (37 of 40) of cells displaying PI fluorescence also display ZCOE fluorescence, based on analysis of eight images (additional images shown in Figure S2). Therefore, it is reasonable to conclude that ZCOE can only enter yeast cells that have compromised membranes. One possible explanation is that its molecular topology, unlike that of DSSN+, cannot find suitable accommodation within and transfer through the lipid membrane due to the additional ionic groups on the center of the molecule. However, due to the negatively charged yeast cell surface²⁶ as in *E. coli*, one would expect some association of ZCOE. In fact, very weak fluorescence is observed near the circumference of cells when the brightness of the image in Figure 2 (top left) is adjusted above the saturation point (Figure S3).

When yeast cells were stained with both COEs at 5 μM (Figure 2, bottom), cells displaying ZCOE fluorescence also exhibit intracellular DSSN+ staining. This is in contrast to the remainder of cells stained with DSSN+ that present a fluorescent “halo” around the circumference of the cells. Indication of lipid membrane intercalation by DSSN+ in these cells is the symmetrically uneven membrane staining pattern, which is similar to what has been observed in liposomal systems with this COE.¹² Regions of attenuated emission run north/south (see arrow in Figure 2, bottom) as a result of the linearly structured chromophore being specifically oriented to span the width of the lipid bilayer. As a result of this alignment, efficient excitation and emission of the chromophore is governed by the direction of polarization of the incident photons, in this case from the polarized 405 nm laser. ZCOE is not expected to orient in a similar manner because ionic groups located on the center of the molecule make it unfavorable for ZCOE to intercalate and remain in the nonpolar region of the lipid bilayer.

As a final point of comparison, COS-1 cells (green monkey kidney cells) were stained with 5 μM ZCOE and DSSN+ for 20 min and imaged both immediately and after ~ 12 h, with the resulting images shown in the top and middle of Figure 3, respectively. Soon after staining, emissions for both ZCOE and DSSN+ exhibit similar localization to both intracellular puncta as well as the plasma membrane. After ~ 12 h, however, ZCOE emission is entirely confined to intracellular groupings of small puncta, while DSSN+ emission both colocalizes with ZCOE and is retained within the plasma membranes. A replicate experiment is shown in Figure S4 and further highlights the retention of DSSN+ in the plasma membrane.

Upon observation of the small, round structures displaying ZCOE emission that were similar to previous work with cationic conjugated polyelectrolytes,²⁷ it was hypothesized that ZCOE was being endocytosed.²⁸ To test this hypothesis, COS-1 cells were stained with 5 μM ZCOE, rinsed and incubated in growth medium for 12 h, and then stained with LysoTracker Green (Figure 3, bottom) to mark acidic cellular compartments associated with endocytosis, such as late endosomes and lysosomes.²⁹ Good colocalization is observed between the two dyes, indicating that some ZCOE is trafficked to these acidic compartments. Further evidence indicating endocytosis is the localization of some ZCOE to late endosomes, marked by Rab7³⁰ and Rab9³¹ proteins (Figures S5 and S6). These observations are consistent with ZCOE being internalized by COS-1 cells via endocytosis, though it does not necessarily rule out other modes of entry.

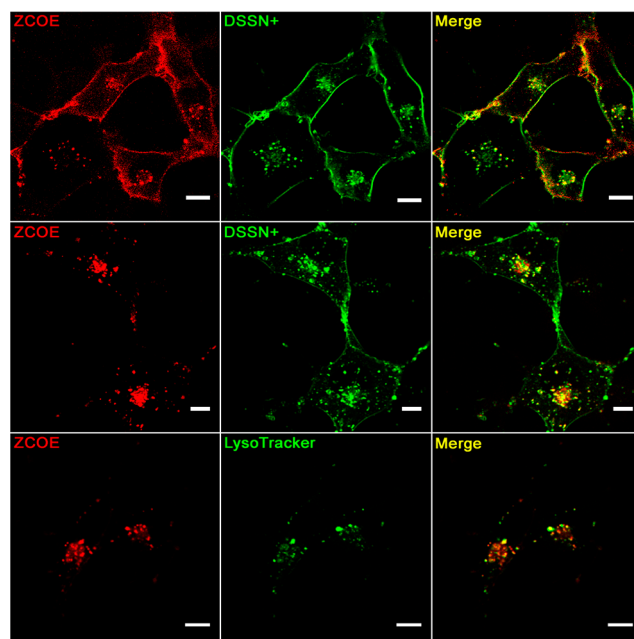


Figure 3. Single-plane confocal micrographs of COS-1 cells stained with 5 μM ZCOE. (Top) Dual stain with 5 μM DSSN+ imaged soon after staining and after ~ 12 h (middle). (Bottom) Dual stain with LysoTracker Green applied 12 h after ZCOE. Scale bars are 10 μm .

In conclusion, we report the synthesis and photophysical characterization of a new COE containing molecular design elements incorporated to differentiate its interaction with biological systems from those of the more established DSSN+. Specifically, DSSN+ contains four long-axis-terminating pendant ionic groups which mimic the distribution of hydrophilic and hydrophobic components of a lipid bilayer, whereas ZCOE contains six evenly distributed pendant ionic groups across its π -conjugated backbone, making it more hydrophilic and less likely to persist in a hydrophobic lipid environment. Consistent with their differing ionic topologies, DSSN+ generally accumulated in lipid membranes, whereas ZCOE exhibited less specific staining patterns, likely governed by electrostatic interactions with cell surfaces. In *E. coli*, ZCOE displays cell-associated emission, most likely as a result of interactions with the negatively charged surface of the bacteria. In yeast, ZCOE similarly associates with the outside of cells but accumulates inside certain cells that, based on dual staining with PI, have compromised membranes. In mammalian cells, emission from ZCOE initially appears similarly to that of DSSN+, most likely due to association with the negatively charged mammalian cell surface,²⁷ but after 12 h all ZCOE fluorescence is confined to intracellular puncta that show a significant degree of colocalization with LysoTracker and other late endosome markers, suggesting it has been subjected to an endocytotic pathway, which is not uncommon for polycationic molecules.^{27,32} The results of these imaging experiments demonstrate the impact that the structural differences of COEs, especially the distribution of ionic groups, can have on their interaction with biological systems.

■ ASSOCIATED CONTENT

📄 Supporting Information

Synthetic procedures, experimental details, bright-field images, and other supporting results. This material is available free of charge via the Internet at <http://pubs.acs.org>.

■ AUTHOR INFORMATION

Corresponding Author

bazan@chem.ucsb.edu

Notes

The authors declare no competing financial interest.

■ ACKNOWLEDGMENTS

This work was supported by the Institute for Collaborative Biotechnologies through grant W911NF-09-0001 from the U.S. Army Research Office. The authors would like to thank the NIH (grant no. 1S10OD010610-01A1) for funding of the confocal microscopy facilities, Dr. A. Mikhailovski for photo-physical characterization, Prof. Dzwokai Ma for GFP-Rab expression vectors, and Dr. Mary Raven for assistance with the confocal microscopy.

■ REFERENCES

- (1) (a) Yang, R.; Xu, Y.; Dang, X.-D.; Nguyen, T.-Q.; Cao, Y.; Bazan, G. C. *J. Am. Chem. Soc.* **2008**, *130*, 3282. (b) *Conjugated Polyelectrolytes Fundamentals and Applications*; Liu, B., Bazan, G. C., Eds.; Wiley-VCH GmbH & Co: Weinheim, 2013.
- (2) Lee, Y.; Yang, I.; Lee, J. E.; Hwang, S.; Lee, J. W.; Um, S.-S.; Nguyen, T. L.; Yoo, P. J.; Woo, H. Y.; Park, J.; Kim, S. K. *J. Phys. Chem. C* **2013**, *117*, 3298.
- (3) Pu, K.-Y.; Li, K.; Zhang, X.; Liu, B. *Adv. Mater.* **2010**, *22*, 4186.
- (4) Ding, D.; Pu, K.-Y.; Li, K.; Liu, B. *Chem. Commun.* **2011**, 47, 9837.
- (5) Song, W.; Jiang, R.; Yuan, Y.; Lu, X.; Hu, W.; Fan, Q.; Huang, W. *Chin. Sci. Bull.* **2013**, *58*, 2570.
- (6) Cai, L.; Zhan, R.; Pu, K.-Y.; Qi, X.; Zhang, H.; Huang, W.; Liu, B. *Anal. Chem.* **2011**, *83*, 7849.
- (7) Hammarström, P.; Simon, R.; Nyström, S.; Konradsson, P.; Åslund, A.; Nilsson, K. P. R. *Biochemistry* **2010**, *49*, 6838.
- (8) Herland, A.; Nilsson, K. P. R.; Olsson, J. D. M.; Hammarström, P.; Konradsson, P.; Inganäs, O. *J. Am. Chem. Soc.* **2005**, *127*, 2317.
- (9) Li, H.; Bazan, G. C. *Adv. Mater.* **2009**, *21*, 964.
- (10) Åslund, A.; Sigurdson, C. J.; Klingstedt, T.; Grathwohl, S.; Bolmont, T.; Dickstein, D. L.; Glimsdal, E.; Prokop, S.; Lindgren, M.; Konradsson, P.; Holtzman, D. M.; Hof, P. R.; Heppner, F. L.; Gandy, S.; Jucker, M.; Aguzzi, A.; Hammarström, P.; Nilsson, K. P. R. *ACS Chem. Biol.* **2009**, *4*, 673.
- (11) Duarte, A.; Chworos, A.; Flagan, S. F.; Hanrahan, G.; Bazan, G. C. *J. Am. Chem. Soc.* **2010**, *132*, 12562.
- (12) Garner, L.; Park, J.; Dyar, S.; Chworos, A.; Sumner, J.; Bazan, G. C. *J. Am. Chem. Soc.* **2010**, *132*, 10042.
- (13) Wang, V. B.; Du, J.; Chen, X.; Thomas, A. W.; Kirchhofer, N. D.; Garner, L. E.; Maw, M. T.; Poh, W. H.; Hinks, J.; Wuertz, S.; Kjelleberg, S.; Zhang, Q.; Loo, J. S. C.; Bazan, G. C. *Phys. Chem. Chem. Phys.* **2013**, *15*, 5867.
- (14) Hou, H.; Chen, X.; Thomas, A. W.; Catania, C.; Kirchhofer, N. D.; Garner, L. E.; Han, A.; Bazan, G. C. *Adv. Mater.* **2013**, *25*, 1593.
- (15) Garner, L. E.; Thomas, A. W.; Sumner, J. J.; Harvey, S. P.; Bazan, G. C. *Energy Environ. Sci.* **2012**, *5*, 9449.
- (16) Thomas, A. W.; Garner, L. E.; Nevin, K. P.; Woodard, T. L.; Franks, A. E.; Lovley, D. R.; Sumner, J. J.; Sund, C. J.; Bazan, G. C. *Energy Environ. Sci.* **2013**, *6*, 1761.
- (17) Du, J.; Thomas, A. W.; Chen, X.; Garner, L. E.; Vandenberg, C. A.; Bazan, G. C. *Chem. Commun.* **2013**, 49, 9624.
- (18) Wang, Y.; Schanze, K. S.; Chi, E. Y.; Whitten, D. G. *Langmuir* **2013**, *29*, 10635.
- (19) Wang, Y.; Chi, E. Y.; Schanze, K. S.; Whitten, D. G. *Soft Matter* **2012**, *8*, 8547.
- (20) Wang, Y.; Corbitt, T. S.; Jett, S. D.; Tang, Y.; Schanze, K. S.; Chi, E. Y.; Whitten, D. G. *Langmuir* **2012**, *28*, 65.
- (21) Ellinger, S.; Graham, K. R.; Shi, P.; Farley, R. T.; Steckler, T. T.; Brookins, R. N.; Taranekekar, P.; Mei, J.; Padilha, L. A.; Ensley, T. R.

Hu, H.; Webster, S.; Hagan, D. J.; Van Stryland, E. W.; Schanze, K. S.; Reynolds, J. R. *Chem. Mater.* **2011**, *23*, 3805.

(22) Turro, N. J. *Modern Molecular Photochemistry*; University Science Books: Sausalito, CA, 1991.

(23) Horie, M.; Kettle, J.; Yu, C.-Y.; Majewski, L. A.; Chang, S.-W.; Kirkpatrick, J.; Tuladhar, S. M.; Nelson, J.; Saunders, B. R.; Turner, M. L. *J. Mater. Chem.* **2012**, *22*, 381.

(24) Hillberg, A. L.; Tabrizian, M. *Biomacromolecules* **2006**, *7*, 2742.

(25) Deere, D.; Shen, J.; Vesey, G.; Bell, P.; Bissinger, P.; Veal, D. *Yeast* **1998**, *14*, 147.

(26) De Nobel, J. G.; Barnett, J. A. *Yeast* **1991**, *7*, 313.

(27) McRae, R. L.; Phillips, R. L.; Kim, I.-B.; Bunz, U. H. F.; Fahrni, C. J. *J. Am. Chem. Soc.* **2008**, *130*, 7851.

(28) Zhu, C.; Liu, L.; Yang, Q.; Lv, F.; Wang, S. *Chem. Rev.* **2012**, *112*, 4687.

(29) Lai, S. K.; Hida, K.; Man, S. T.; Chen, C.; Machamer, C.; Schroer, T. A.; Hanes, J. *Biomaterials* **2007**, *28*, 2876.

(30) Misaki, R.; Nakagawa, T.; Fukuda, M.; Taniguchi, N.; Taguchi, T. *Biochem. Biophys. Res. Commun.* **2007**, *360*, 580.

(31) Gong, Q.; Huntsman, C.; Ma, D. J. *Cell. Mol. Med.* **2008**, *12*, 126.

(32) Joliot, A.; Prochiantz, A. *Nat. Cell Biol.* **2004**, *6*, 189.